

Controllable Synthesis of Cu₂S Nanocrystals and Their Assembly into a Superlattice

Zhongbin Zhuang, Qing Peng,* Boce Zhang, and Yadong Li*

Department of Chemistry, Tsinghua University, Beijing, 100084 People's Republic of China

Received May 15, 2008; E-mail: pengqing@mail.tsinghua.edu.cn; ydli@mail.tsinghua.edu.cn

Monodisperse nanocrystals referred as “artificial atoms” can “bottom-up” assemble into a nanocrystal superlattice. Large-scale multilayer superlattices exhibit significant, tunable collective physical and chemical properties.^{1,2} It is the basis for the nanomaterials and nanodevices in the future. The design and construction of a nanocrystal superlattice have attracted great interests in fundamental as well as applied research areas. To reach this goal, the building block nanocrystals should be quite uniform in size and shape, while it is still a challenge for material scientists. In this communication, we report an attempt on the synthesis of highly uniform Cu₂S nanocrystals with controllable size and shape, as well as their multilayer superlattice assemblies. This work will provide a new bottom-up approach to synthesize and integrate nanocrystals, as well as their properties, which has potential applications such as thin film fabrications in solar cells.

Chalcocite (Cu₂S) is a p-type semiconductor with a bulk band gap of 1.2 eV and has wide applications in solar cells,³ cold cathodes,⁴ and nanoscale switches,⁵ etc. Cu₂S has an anisotropic hexagonal crystal structure, and the arrangement of atoms along the *c*-axis is quite different from the others. Thus it is possible to adjust the growth rate along [001] and [100] directions to obtain plate-like nanocrystals with different diameter/thickness ratios. This allows the possibility to tailor the nanocrystal's shape and further engineer the packing symmetry of the superlattice. The anisotropic structure also has a dipole moment along the [001] direction, which may be useful for the stacking of nanocrystals in the construction of superlattices.

Korgel and co-workers have reported a pioneer work on the synthesis of Cu₂S nanoplates through a solventless method and have investigated their columnar assemblies.⁶ Their results show the possibility to construct multilayer superlattices if the nanocrystals are extraordinarily uniform. Herein, we develop a novel water–oil interface confined method to synthesize monodisperse Cu₂S nanocrystals and their multilayer superlattice assemblies. In our two-phase reaction system, dodecanethiol (or its toluene solution) is the upper oil phase, which plays the roles of sulfur source, ligand, and reducer. The lower aqueous phase contains copper ion and other added anions (Ac[−] or Cl[−], used as ligands for adjusting the growth of Cu₂S). The synthesis was performed in an autoclave at 200 °C. The Cu₂S nanocrystals formed at the interface of water and dodecanethiol and were capped by dodecanethiol molecules. The hydrophobic shell and the water–oil interface may help the nanocrystals self-assemble into advanced structures. The experimental details are shown in the Supporting Information.

Figure 1 shows the TEM images of the as-obtained Cu₂S nanocrystals. Figure 1a shows the products obtained in the presence of Ac[−]. They are circular in shape with a narrow size distribution (Figure 1b) and a diameter of 8.2 ± 0.7 nm. The HRTEM image (Figures 1c and S1b) shows the lattice fringes, which can be indexed as the (110) plane. This indicates that the nanocrystal is terminated by the {001} plane. Figure 1d–f shows the products obtained under lower concentration of Cu²⁺ and dodecanethiol. In this case, the nanocrystals changed from circular shape to an elongated shape but remain uniform (Figure 1e).

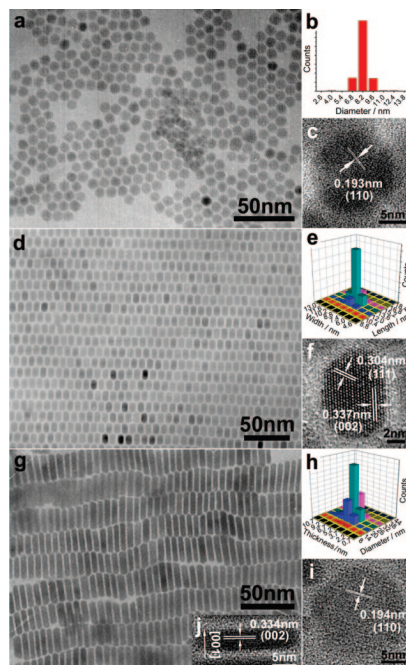


Figure 1. TEM images of the as-obtained Cu₂S nanocrystals: TEM image (a), size distribution (b), and HRTEM image (c) of circular Cu₂S nanocrystals; TEM image (d), size distribution (e), and HRTEM image (f) of elongated Cu₂S nanocrystals; TEM image (g), size distribution (h), and HRTEM image (i, j) of Cu₂S hexagonal nanoplates. Enlarged size distribution patterns and clearer HRTEM images are shown in Figure S1 in Supporting Information.

The length of the elongated nanocrystal is 13.6 ± 0.8 nm with a width of 8.8 ± 0.7 nm. The HRTEM image (Figures 1f and S1d) shows the good crystallinity, and the lattice fringes can be indexed as (11̄1) and (002). Different from the former product, the side face of the elongated nanocrystal is the {001} plane. Figure 1g–j shows the product obtained in the presence of Cl[−] (a stronger ligand than Ac[−]). They seem like close-packed nanorods. However, from the face-down object and overlap of the nanocrystals in the sample (Figure S2), it was found that they are face-to-face packed hexagonal nanoplates in nature. The thickness of the nanoplate is 5.2 ± 0.9 nm with a diameter of 26 ± 4 nm. They have a wider size distribution (Figure 1h), which makes them not as good as the formers for the construction of multilayer superlattices. The HRTEM images (Figures 1i, j, S1f, and S1g) show that the nanoplate lies on the {001} plane, which is in agreement with the literature.⁶

Figure S2 shows the XRD patterns of the above-mentioned samples, in which a set of peaks can be indexed as pure hexagonal Cu₂S structure (JCPDS card No. 84-0208). By controlling the reaction rate (including the nucleation and growth rates), the sizes and shapes of nanocrystals can be engineered. Ac[−] is a weak ligand and has less effect on Cu²⁺, so the reaction rate in this case is the fastest. This results in forming small size circular nanocrystals. By diluting

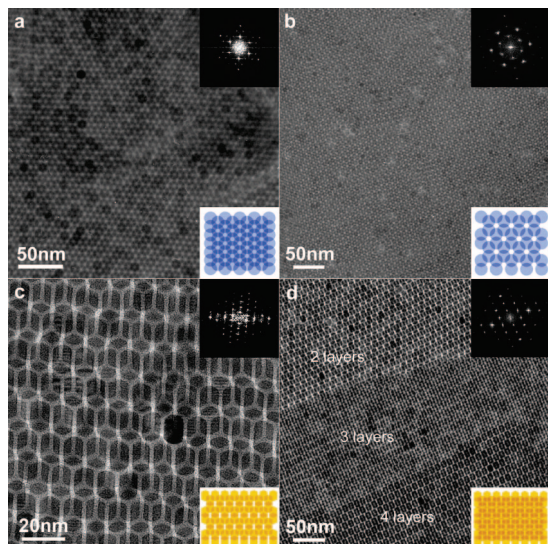


Figure 2. TEM images of Cu_2S nanocrystal assemblies: (a) fcc packed circular nanocrystals; (b) hcp packed circular nanocrystals; (c) two layers of close-packed elongated nanocrystals; (d) multilayers of elongated nanocrystals. The top insets are the corresponding FFT patterns, and the bottom insets are the schemes of the stacking of nanocrystals. Detailed schemes and descriptions of the packing symmetry of nanocrystals are shown in Figure S4.

dodecanethiol with toluene to slow the reaction rate, elongated nanocrystals were obtained. By replacing Ac^- with a stronger ligand Cl^- (to form CuCl_4^{2-} and lead to the slowest reaction rate), the as-obtained nanocrystals are hexagonal nanoplates. They are different in shape from the circular and elongated ones with a large size.

The above-mentioned circular and elongated nanocrystals both have strong tendency to assemble into multilayer superlattices because of their high uniformity. The nanocrystal superlattices are formed spontaneously during the preparation stage. Figure 2 shows the TEM images of the nanocrystal assemblies. The circular nanocrystals can close pack into a layer, and the second-layer nanocrystals fit into the voids between the first-layer nanocrystals. Two types of packing symmetry can be adopted by the third-layer nanocrystals to build fcc (Figure 2a) or hcp (Figure 2b) superlattices. The inset FFT patterns show the high stacking order with a sixth-fold axis. The ordering over a distance is up to hundreds of nanometers. They are 3D stacking superlattices but provide the best imaging when the sample is 3–10 layers thick. Some faceted superlattices are also found in our sample. Figure S5 displays the (111) projection of a faceted fcc-type superlattice and results in a triangular morphology.

It was observed that the orientation of the atomic lattice of an individual nanocrystal packed into a superlattice is not random. They have a preferred orientation that can be studied by selected area electron diffraction (SAED, Figure S6). It displays six symmetrical arcs but not uniform diffraction rings. This indicates the building block nanocrystals are oriented along [001] and the inner nanocrystals are deviated from spheres⁷ with circular tablet-like shape.

When the nanocrystals are elongated, the stacking of the nanocrystals still holds the close-packed form. The upper layer nanocrystals can also fit into the voids between the lower layers, thus forming a multilayer structure (Figure 2c,d). As stated in the previous case, the SAED pattern (Figure S7) also shows the preferred orientation of the elongated nanocrystal assemblies. However, the nanocrystals are oriented along [110] instead of the [001] of circular nanocrystal assemblies. The hexagonal nanoplates form a discotic phase, which

includes columnar assemblies. This type of assembly has strong interactions within the column but weak between columns.

Entropy drives the nanocrystals into a superlattice when the nanocrystals have large volume fractions.² Furthermore, the dipole–dipole and van der Waals interactions also promote the nanocrystal to assemble. The anisotropic cell structure of Cu_2S leads to a dipole moment along the [001] direction of those nanocrystals, and this may also be useful for the stacking of building blocks⁸ (the detailed discussion is shown in Figure S8 of the Supporting Information). Because of the different orientation of the inner nanocrystals in the superlattice, the dipole moment orientations are different in the two types of nanocrystal superlattices. It is vertical to the layers in the case of circular nanocrystal assemblies, which may lead to a strong tendency to form a multilayer structure. However, in the elongated nanocrystal assemblies, the dipole moment is along the side face of the nanocrystals. The van der Waals interactions depend on the distance of the two species strongly, and the elongated nanocrystal may have larger “closest regions” and result in larger interactions (Figure S9 in the Supporting Information).

In conclusion, highly uniform Cu_2S nanocrystals have been synthesized through a simple water–oil interface confined reaction. They can self-assemble into highly ordered multilayer superlattices. By controlling the size and shape of the building block nanocrystals, it shows the possibility to adjust the packing symmetry of the superlattice and further to tailor the structures and performances of the assemblies. This work provides a simple bottom-up approach to integrate nanocrystals, as well as their properties, which may have potential applications for nanomaterials and nanodevices in the future.

Acknowledgment. This work was supported by NSFC (90606006, 20771064), the State Key Project of Fundamental Research for Nanoscience and Nanotechnology (2006CB932303, 2006CB932608), and Tsinghua Basic Research Foundation.

Supporting Information Available: Experiment details, enlarged size distribution pattern, magnified HRTEM, additional TEM, XRD, SAED results, and discussion of the interactions. This material is available free of charge via the Internet at <http://pubs.acs.org>.

References

- (1) (a) Alivisatos, A. P. *Science* **1996**, *271*, 933. (b) Murray, C. B.; Kagan, C. R.; Bawendi, M. G. *Annu. Rev. Mater. Sci.* **2000**, *30*, 545. (c) Burda, C.; Chen, X. B.; Narayanan, R.; El-Sayed, M. A. *Chem. Rev.* **2005**, *105*, 1025. (d) Wang, X.; Zhuang, J.; Peng, Q.; Li, Y. D. *Nature* **2005**, *437*, 121. (e) Yin, Y.; Alivisatos, A. P. *Nature* **2005**, *437*, 664.
- (2) (a) Murray, C. B.; Kagan, C. R.; Bawendi, M. G. *Science* **1995**, *270*, 1335. (b) Li, M.; Schnablegger, H.; Mann, S. *Nature* **1999**, *402*, 393. (c) Markovich, G.; Collier, C. P.; Henrichs, S. E.; Remacle, F.; Levine, R. D.; Heath, J. R. *Acc. Chem. Res.* **1999**, *32*, 415. (d) Kalsin, A. M.; Fialkowski, M.; Paszewski, M.; Smoukov, S. K.; Bishop, K. J. M.; Grzybowski, B. A. *Science* **2006**, *312*, 420. (e) Shevchenko, E. V.; Talapin, D. V.; Kotov, N. V.; O'Brien, S.; Murray, C. B. *Nature* **2006**, *439*, 55. (f) Zhuang, Z. B.; Peng, Q.; Wang, X.; Li, Y. D. *Angew. Chem., Int. Ed.* **2007**, *46*, 8174. (g) Pileni, M. P. *Acc. Chem. Res.* **2007**, *40*, 685.
- (3) Lee, H.; Yoon, S. W.; Kim, E. J.; Park, J. *Nano Lett.* **2007**, *7*, 778.
- (4) Chen, J.; Deng, S. Z.; Xu, N. S.; Wang, S. H.; Wen, X. G.; Yang, S. H.; Yang, C. L.; Wang, J. N.; Ge, W. K. *Appl. Phys. Lett.* **2002**, *80*, 3620.
- (5) Chen, L.; Xia, Y. D.; Liang, X. F.; Yin, K. B.; Yin, J.; Liu, Z. G.; Chen, Y. *Appl. Phys. Lett.* **2007**, *91*, 073511.
- (6) (a) Larsen, T. H.; Sigman, M.; Ghezelbash, A.; Doty, R. C.; Korgel, B. A. *J. Am. Chem. Soc.* **2003**, *125*, 5638. (b) Sigman, M. B.; Ghezelbash, A.; Hanrath, T.; Saunders, A. E.; Lee, F.; Korgel, B. A. *J. Am. Chem. Soc.* **2003**, *125*, 16050. (c) Saunders, A. E.; Ghezelbash, A.; Smilgies, D. M.; Sigman, M. B.; Korgel, B. A. *Nano Lett.* **2006**, *6*, 2959.
- (7) Wang, Z. L. *J. Phys. Chem. B* **2000**, *104*, 1153.
- (8) (a) Tang, Z. Y.; Kotov, N. A.; Giersig, M. *Science* **2002**, *297*, 237. (b) Talapin, D. V.; Shevchenko, E. V.; Murray, C. B.; Titov, A. V.; Kral, P. *Nano Lett.* **2007**, *7*, 1213.

JA803644G